

Effect of interface roughness and well width on differential reflection dynamics in InGaAs/InP quantum wells

Y.-G. Zhao,^{a)} Y.-H. Zou, J.-J. Wang, Y.-D. Qin, and X.-L. Huang

Department of Physics and Mesoscopic Physics Laboratory, Peking University, Beijing 100871, People's Republic of China and National Laboratory for Superlattices and Microstructures, Beijing 100083, People's Republic of China

R. A. Masut and A. Bensaada

Groupe de Recherche en Physique et Technologie des Couches Minces (GCM) et Département de Génie Physique, Ecole Polytechnique de Montréal, C. P. 6079, Succ. Centre-Ville, Montréal, Québec H3C 3A7, Canada

(Received 29 April 1997; accepted for publication 4 November 1997)

We have observed differential reflection dynamics in $\text{In}_{0.518}\text{Ga}_{0.492}\text{As}/\text{InP}$ multiple quantum wells, using the pump-probe technique, and examined the photoluminescence spectra to determine the interface quality for the samples studied. Our results show that the interface quality and well width of the quantum wells (QWs) strongly influence the differential reflection dynamics. The experimental results provide a direct evidence to demonstrate that photoexcited carrier diffusion in cap layer and barriers along the direction perpendicular to sample surface plays a dominant role in determining the differential reflection dynamics of the QWs. © 1998 American Institute of Physics. [S0003-6951(98)04601-4]

The abruptness of quantum well (QW) heterointerfaces can greatly influence the properties of heterostructure devices. For a thin QW with a rough heterointerface, the photoluminescence (PL) line width increases¹ and electron mobility decreases.² The pump-probe technique provides a powerful experimental method for determining time-resolved relaxation in photoexcited semiconductor materials. It has been widely used to study photoexcited carrier dynamics. However, to our knowledge the study on the effect of interface roughness and well width of QWs on the differential reflection dynamics is lacking.

InGaAs/InP QWs have attracted much attention because of its important technological role in the fabrication of optoelectronic devices. This material system allows the energetic adjustment of radiative transition to the wavelength of minimal absorption ($1.55\ \mu\text{m}$) and zero dispersion ($1.3\ \mu\text{m}$) of commercial silica optical fibers. The optoelectronic properties and material growth of InGaAs/InP QWs have been reported. Some authors have used upconversion PL techniques to study photoexcited carrier capture, thermalization, cooling, and charge transfer from the barriers into wells in InGaAs/InP quantum wells.^{3,4} In this letter, we report the first observation of the differential reflection dynamics in $\text{In}_{0.518}\text{Ga}_{0.482}\text{As}/\text{InP}$ multiple quantum wells (MQWs). The effect of interface roughness and well width on the differential reflection dynamics has been investigated.

The samples studied were grown by metalorganic chemical vapor deposition (MOCVD). We have studied three types of InGaAs/InP MQWs. Sample Nos. 1 and 2 have the same structure, but have different interface qualities since different interruption times were taken for each alloy during MOCVD growth. They consist of a *S*-doped InP substrate, followed by a $2000\ \text{\AA}$ InP undoped buffer layer, $10\ \text{period}\ 70\ \text{\AA}\ \text{In}_{0.518}\text{Ga}_{0.492}\text{As}/400\ \text{\AA}\ \text{InP}$ QWs in the center,

and finally by a $1600\ \text{\AA}$ InP cap layer. Sample No. 3 consists of five wells with different widths $160, 120, 90, 70,$ and $50\ \text{\AA}$, each being separated by a $400\ \text{\AA}$ barrier layer of InP, and the thickness of the cap layer is the same as the sample Nos. 1 and 2. The wells are positioned in the order of decreasing width with distance from the front surface.

Our measurements of differential reflection dynamics were made at room temperature, using the pump-probe technique. The short pulse source was a mode-locked hybrid dye laser synchronously pumped by a frequency-doubled mode-locked yttrium-aluminum-garnet (YAG) laser. The laser produced pulses as short as $150\ \text{fs}$ with a repetition rate of $76\ \text{MHz}$, and around $647\ \text{nm}$ wavelength. The laser beam was split into pump and probe beams. They were orthogonally polarized. The pump beam was normally incident and the probe beam was with an incident angle of 15° . The two beams were focused to an $\sim 20\ \mu\text{m}$ diameter spot on the samples. The probe beam was delayed by a step-motor-drive delay stage. The reflection signals were detected, using a photodiode and a lock-in amplifier. Each data point were represented by the average of several runs over the chosen delay range.

Figure 1 shows differential reflection dynamics measured on the sample Nos. 1, 2, and 3. A distinct fast rising edge, followed by a slow decay has been observed in every sample. However, the time constants of the decay are quite different for different samples. The delay time of sample No. 1 is much longer than those of sample Nos. 2 and 3. In the period of the first $30\ \text{ps}$, the differential reflection signal of sample No. 2 is similar to that of sample No. 1, and after that the decay becomes fast. The decay of sample No. 3 is faster than those of sample Nos. 1 and 2.

We have also determined the PL spectra for the samples studied. The PL measurements were performed using an Ar^+ laser with $5145\ \text{\AA}$ line. The signal was dispersed by a $1\ \text{m}$ spectrometer and detected by a liquid-nitrogen-cooled Ge *p-i-n* photodiode using conventional lock-in techniques.

^{a)}Electronic mail: yiguang@ibm320h.phy.pku.edu.cn

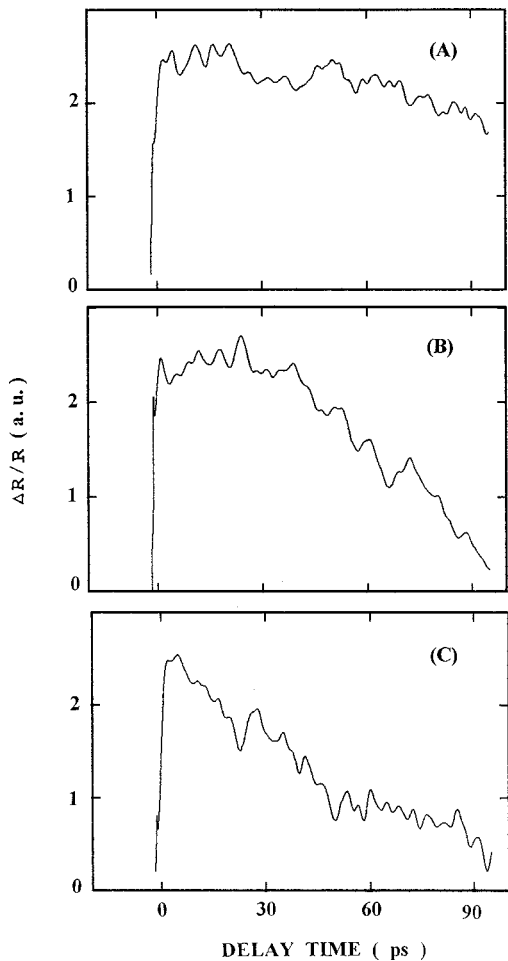


FIG. 1. Time-resolved differential reflection ($\Delta R/R$) measured for different samples (A): sample No. 1; (B): sample No. 2; and (C): sample No. 3.

The sample temperature was maintained in a continuous flow helium cryostat. All PL spectra were measured at 8 K.

Curves A, B, and C shown in Fig. 2 are the PL spectra for sample Nos. 1, 2, and 3, respectively. The PL spectrum of sample No. 1 in the structure is quite different from those of sample Nos. 2 and 3, having only one broad lobe (total linewidth is ~ 62 meV) with a shoulder at high energy side. Curve B has two peaks, and their line widths are ~ 32 and ~ 10 meV, respectively. Curve C has three peaks, one dominant peak (line width is ~ 12 meV) and two small peaks. Using the envelope function approximation,⁵ we have made a calculation to fit the excitonic peak energy position with the PL spectra. The high-energy shoulder of curve A and high-energy peak of curve B are the transition (E_{1H}) between the $n=1$ electron subband and the $n=1$ heavy-hole subband in sample Nos. 1 and 2, respectively; the dominant peak of curve C is the E_{1H} transition in the 160 Å well of sample No. 3. The low-energy features of curves A and B are probably due to the participation of impurities in the recombination process, which is consistent with the situation observed in GaInAs bulk, where all PL has been identified as impurity assisted luminescence,⁶ and similar PL spectra in $\text{Ga}_{0.47}\text{In}_{0.53}\text{As}/\text{InP}$ QWs have also been observed.⁷ The two small peaks of curve C probably are luminescence from the narrower wells.

Interface roughness has a great influence upon the PL

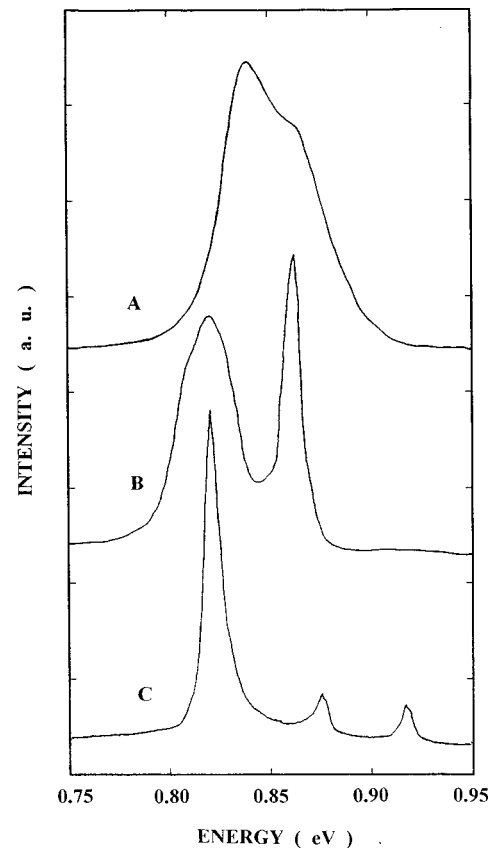


FIG. 2. PL spectra measured for different samples A: sample No. 1; B: sample No. 2; and C: sample No. 3. All PL spectra were measured at 8 K.

line width for the narrow wells; however, the PL line width of the wide wells is relatively insensitive to interface roughness.⁸ For sample No. 3 the widths of the wells located at near sample surface are much wider than those of sample Nos. 1 and 2, thus it has narrower PL line width. The broader PL linewidth of sample No. 1 shows that its interface is rougher than that of sample No. 2.

The evolution of the differential reflection dynamics following the excitation of laser pulse is determined by the changes of the refractive index and the absorption in the cap layer, the wells, and the barriers, and mainly is a consequence of a decrease of the photoexcited carrier density. We have studied the differential reflection dynamics in InGaP/InP film and have demonstrated that the delay time of the differential reflection dynamics depends on the photoexcited carrier diffusion along the direction perpendicular to the film surface.⁹ For the QWs, the photoexcited carrier transfer processes are more complex. When the samples are excited by a laser pulse, the distribution of the carrier density reduces exponentially along the direction perpendicular to the sample surface (z direction). Following the light excitation, the photoexcited carriers will diffuse from high density region to lower density region in the cap layer and the barriers; a fraction of the carriers will be captured by the wells and radiative recombination will occur in the wells, these also induce a density gradient of photoexcited carriers in the barriers, and influence carrier diffusion; and some of the carriers will escape from the wells into the barriers due to thermal emission;¹⁰ the carriers emitted by the wells near surface are transferred across the barriers and can be captured by the

wells located at far from the surface. Previous experimental results show the radiative recombination lifetime of InGaAs/InP QWs are functions of temperature and the thickness of barrier or well, and is much longer than the delay times shown in Fig. 1.¹¹ So that, the influence of the radiative recombination on the differential reflection dynamics can be neglected. We also ignore carrier depletion due to recombination in the cap and barrier layers, and the sample surface. Because the former is justified by the fact that the bulk recombination time is considerably longer than the delay time shown in Fig. 1,¹² the latter is valid provided by the surface recombination velocity $S_n \ll (D/\tau)^{1/2}$, where D is the ambipolar diffusivity. The measured value of S_n for hole in InP is typically $\sim 10^2$ cm/s,¹² while $(D/\tau)^{1/2}$ is estimated to be $\sim 10^5$ cm/s.¹¹ If we take the origin of the z axis at the sample surface, the initial density distribution of photoexcited carriers along the z direction can be expressed by $n(z) = n_0 \exp(-\alpha z)$, where n_0 is the initial carrier density at $z=0$, α is the absorption coefficient and approximates to $\sim 4 \mu\text{m}^{-1}$ for the excited wavelength.¹³ While, the laser beam was focused to an $\sim 20 \mu\text{m}$ diameter spot on the sample as mentioned above. Assume the laser intensity distribution on the sample surface obeys a Gaussian function, thus the density gradient of photoexcited carriers along the z direction is much greater than that in the x - y plane. Therefore, the differential reflection dynamics is mainly determined by the process of photoexcited carrier transport along the z direction. It should be mentioned that after laser excitation the evolution of the photoexcited carrier density in the cap layer and the barriers are different from those in the wells. In the cap layer and in the barriers the carrier density decreases; while, in the wells the carrier density increases at the beginning of just off pump beam pulse, which has different temporal evolution from that of the differential reflection dynamics shown in Fig. 1. Since the thicknesses of the cap layer and the barriers are much larger than those of the wells for samples studied, we propose that carriers diffusion in the cap layer and the barriers along the z direction plays a dominant role in determining the differential reflection dynamics.

Using the above proposition, our experimental results can be satisfactorily explained. The capture efficiency is expressed by¹¹

$$\eta = 1 - \exp(-d_w / \tau_b v_b), \quad (1)$$

where d_w is the well width, τ_b is the trapping time, and v_b is the mean drift velocity of the carriers. For sample No. 3, the width of the wells located at near sample surface is much larger than those of sample Nos. 1 and 2. So, sample No. 3 has a larger capture efficiency. The larger the capture efficiency, the larger the gradient of the photoexcited carrier density in the barriers, and the faster is the carrier diffusion giving rise to a shorter delay time of the differential reflection dynamics. Interface roughness in a silicon metal-oxide-semiconductor field-effect transistor was considered to be inherent to space-charge layers and was expected to constitute a major cause of scattering, especially at high electron concentrations;¹⁴ and the interface roughness scattering dominates the low temperature mobility of two-dimension electrons in QWs.² In our case, the interface roughness scattering will reduce the diffusion velocity of photoexcited car-

riers in the cap layer and the barriers, resulting a longer delay time of the differential reflection dynamics. The interface quality of sample No. 1 is rougher than that of sample No. 2, so that its delay time of the differential reflection dynamics is longer than that of sample No. 2 as shown in Fig. 1. We have also measured some samples with the same interface qualities as that of sample No. 1, and same results have been observed.

We have studied the differential reflection dynamics in $\text{InAs}_x\text{P}_{1-x}/\text{InP}$ ($x \leq 0.35$) strained-MQWs. Our experimental results show that for the QWs with same interface quality and well width, their delay times of the differential reflection dynamics decrease with increasing arsenic composition. We have also used the above proposition to explain the barrier height dependence of the differential reflection dynamics. Our calculated results show that the smaller the barrier height, the more carriers escape from the wells into the barriers due to thermal emission, which will reduce the mobility of photoexcited carriers because of carrier-carrier scattering inducing a longer decay of the differential reflection dynamics. The results will be published elsewhere.

In conclusion, the above experimental results provide a direct evidence to demonstrate that photoexcited carrier diffusion in the cap layer and the barriers along the direction perpendicular to the sample surface plays a dominant role in determining the differential reflection dynamics of the samples studied. For the QWs with poor interface quality, carrier diffusion velocity in the barriers will be decreased because of interface roughness scattering, which will cause a longer delay time of the differential reflection dynamics; for the QWs with larger well width, the larger capture efficiency is expected, which will induce a larger gradient of the photoexcited carrier density in the barriers, thus the velocity of the carrier diffusion in the barriers will be accelerated, resulting a shorter delay time of the differential reflection dynamics.

¹J. Singh and K. K. Bajaj, J. Appl. Phys. **57**, 5433 (1985).

²H. Sakaki, T. Noda, K. Hirakawa, M. Tanaka, and T. Matsusue, Appl. Phys. Lett. **51**, 1934 (1987).

³B. Deveaud, J. Shah, T. C. Damen, and W. T. Tsang, Appl. Phys. Lett. **50**, 1886 (1988).

⁴R. Kersting, R. Schwedler, K. Wolter, K. Leo, and H. Kurz, Phys. Rev. B **46**, 1639 (1992).

⁵G. Bastard, Phys. Rev. B **24**, 5693 (1981).

⁶Y.-S. Chen and O. K. Kim, J. Appl. Phys. **52**, 7392 (1981).

⁷M. Razeghi, J. P. Hirtz, U. O. Ziemelis, C. Delalande, B. Etienne, and M. Voos, Appl. Phys. Lett. **43**, 585 (1983).

⁸J. Singh and K. K. Bajaj, J. Appl. Phys. **57**, 5433 (1985).

⁹Y. G. Zhao, R. Jing, Y.-H. Zou, Z.-J. Xia, X.-L. Huang, W.-X. Chen, and R. A. Masut, Appl. Phys. Lett. **68**, 696 (1996).

¹⁰H. Schneider and K. V. Klitzing, Phys. Rev. B **38**, 6160 (1988).

¹¹D. J. Westland, D. Mihailovic, J. F. Ryan, and M. D. Scott, Appl. Phys. Lett. **51**, 590 (1987).

¹²V. Diadiuk, S. H. Groves, C. A. Armiento, and C. E. Hurwitz, Appl. Phys. Lett. **42**, 892 (1983).

¹³K.-H. Hellwege, M. Schulz, and H. Weiss, in *Landolt-Bornstein, Numerical Data and Functional Relationship in Science and Technology* (Springer, Berlin, 1982), Vol. 17, Subvol. A.

¹⁴T. Ando, A. B. Fowler, and F. Stern, Rev. Mod. Phys. **54**, 437 (1982).